Ali *et al.*
Bulletin of the National Research Centre (2022) 46:274
https://doi.org/10.1186/s42269-022-00963-1

Bulletin of the National Research Centre

RESEARCH

Open Access

The targeted delivery of chitosan nanoparticles to treat indoxacarb: induced lung fibrosis in rats

Naglaa A. Ali[1*], Mohamed S. Kishta[1], Mohamed Fekry[2] and Safaa H. Mohamed[1]

Abstract

Background: This study evaluated the effects of chitosan nanoparticles (Ch-NPs) on indoxacarb (INDOX)-induced pulmonary fibrosis in in vivo and in vitro models. In in vivo studies, 40 male albino rats were randomly divided into four groups (10 rats/group): Group 1, normal control; Group 2, INDOX (600 mg/kg b.w.); Group 3, Ch-NPs (2 mg/kg b.w.); and Group 4, Ch-NPs + INDOX. Characterization of Ch-NPs was done measuring dynamic light scattering, zeta potential, Fourier-transform infrared spectroscopy, transmission electron microscopy, and antioxidant activity studies after various Ch-NPs treatments. From in vitro studies, the impact of Ch-NPs on A549 lung carcinoma cell proliferation was also examined.

Results: Our data indicated that INDOX provoked considerable lung damage as indicated by decreased antioxidant enzyme levels of superoxide dismutase and glutathione peroxidase, increased production of nitric oxide and malondialdehyde serum levels, elevated myeloperoxidase activity, increased hydroxyproline and cytokeratin-19 serum levels, and significantly upregulated matrix metallopeptidase-9 and microRNA-101 gene expression levels when compared with controls. Furthermore, histopathological and immunohistochemical investigations of cyclooxygenase-2 in the lung tissue revealed marked inflammation, severe fibrosis, and neutrophil infiltration. Critically, Ch-NPs treatment significantly reversed INDOX-induced changes in lung biochemical, histopathological, and immunohistochemical outcomes.

Conclusion: Therefore, Ch-NPs may function as potential therapeutic drugs for lung fibrosis owing to their antioxidant, anti-inflammatory, and antifibrotic activities with neutrophil infiltration.

Keywords: Chitosan nanoparticles, Indoxacarb, Lung fibrosis, Oxidative stress, Inflammation

Background

Pulmonary fibrosis (PF) is the most common fibrotic lung disease, which has a poor prognosis and high mortality rate (Du Bois 2010). Disease pathogenesis involves abnormal reepithelialization, elevated fibroblast proliferation, and unregulated extracellular matrix accumulation following alveolar damage, which leads to progressive respiratory fibrosis and lung failure (Wynn and Ramalingam 2012). In addition, in several animal models, oxidative stress has been identified in animals suffering from lung fibrosis, with aberrant antioxidant activity exacerbating PF (Kliment and Oury 2010). While several drugs have been approved for PF treatment, e.g., pirfenidone, in Japan and Europe (Moran 2011), more novel and promising effective therapeutics for PF are required.

Pesticides are chemicals that prevent, destroy, repel, or mitigate pests, ranging from insects to microorganisms (Alavanja 2009). Humans are often exposed to pesticides due to environmental contamination or practical uses (Bolognesi 2003). Furthermore, every year, more

*Correspondence: almardeyah@gmail.com

[1] Hormones Department, Medical Research and Clinical Studies Institute, National Research Centre, 33-El-Bohouth St. (Former El-Tahrir St.), Dokki, Giza P.O 12622, Egypt
Full list of author information is available at the end of the article

than three million cases of pesticide poisoning occur, which results in more than 250,000 deaths (Hock and Lorenz 2006). Indoxacarb (INDOX) is an oxadiazine pesticide commonly used to control insect resistance to carbamates, organophosphates, and pyrethroids; its main mode of action is the blocking of voltage-dependent sodium channels (Shit et al. 2008). INDOX is also a pro-pesticide that undergoes bioactivation to N-decarbomethoxylated metabolites, which are much more toxic than the parent compound. It is moderately toxic to rats and is classified as category II according to acute oral toxicity levels (CEPA 2004). In the studies of acute inhalation, lung damage was caused by INDOX; "lung noise" indicates the development of acute lung fibrosis injury and elevated pulmonary edema, suggesting that oxidants are generated during INDOX metabolism (U.S. EPA. 2007).Thus, safe and effective treatments for pesticide poisoning are urgently required.

Nanotechnology is promising for the development of targeted drug delivery systems (Kerch 2015). Chitosan is considered a unique, naturally occurring renewable polysaccharide produced via chitin deacetylation. Chitin is found in several natural sources, including crustacean exoskeletons, e.g., crabs, shrimps, and lobsters, insects, and also mollusks and fungi (Luo and Wang 2013). The small chitosan nanoparticles (Ch-NPs) size allows them to pass through in vivo biological barriers, such as the blood–brain barrier (Joshi et al. 2010). Their biological application depends on the molecular weight and deacetylation levels (Zheng et al. 2013). Ch-NPs have several biological activities including, antitumor, anti-inflammatory, and antifungal activities, immune-enhancing effects, drug carrier functions (Yang et al. 2009), antioxidant properties, lipid-lowering activities, and antimicrobial capacities (Mazzotta et al. 2019). The ionic gelation method depends on the ionic interactions between positive charges on the chitosan surface and negative charges on the surface of the cell receptors, sodium tripolyphosphate (TPP), and it hydrolyzes into simpler phosphates that act as nutrients. Ch-NPs toxicity is very low (Lee et al. 2016a, b). The size and charge of chitosan–tripolyphosphate nanoparticles (Ch-NPs) have important roles in determining its biological behavior, e.g., cellular uptake and protein adsorption. Ch-NPs have been utilized for nontoxicity, biocompatibility, and biodegradability purposes (Cheung et al. 2015), and for the removal of heavy metals from contaminated water (Hussein et al. 2012).

Therefore, we investigated the biological implication of synthetic Ch-NPs in lung fibrosis models induced by excessive doses of INDOX.

Methods

Chemicals and reagents

Indoxacarb (Avaunt®, 15% SC) was supplied by Syngenta Agro Services AG, Egypt. Characterization of Ch-NPs was done, and sodium hydroxide, hydrochloric acid, acetone, and TPP were purchased from Sigma-Aldrich Chemical Co., St. Louis, MO, USA.

Ch-NPs preparation

The Ch-NPs nanoparticles were prepared via the ionic interaction between a positively charged amino group $(NH_3)^+$ on chitosan and $(P_3O_{10})^{5-}$anions. Shrimp shells were collected and dispersed in water. The temperature was increased to 90 °C to remove soluble organics, adhesion proteins, and other impurities. Subsequently, the shells were dried at 70 °C for 24 h and then treated with 3.5% (w/w) sodium hydroxide solution for 3 h at 70 °C with stirring; the shell to sodium hydroxide solution ratio was 1:10 (w/v). After 2 h, the mixture was filtered, and the solid mass was washed several times in distilled water for 40 min. Demineralization was conducted by soaking the shells in 1 N hydrochloric acid (HCl) for 24 h at room temperature and maintaining the shell/HCl ratio at 1:15 (w/v). The solution was then filtered under vacuum, and the treated shells (500 g) were washed with distilled water and rinsed in 50% sodium hydroxide solution at 100 °C for 2 h. Subsequently, the shells were washed with distilled water until neutralized and then filtered and dried at 70 °C for 12 h. The treated shells were approximately 20% by weight of shells before treatment (Yang et al. 2009).

Synthesis of Ch-NPs

The prepared solid chitosan was dissolved in 1% acetic acid solution, heated to 70 °C for 3 h with vigorous stirring, and filtered. Then, the TPP (0.1%) solution was slowly added in an equal volume. The final pH was 5.7. The solution was vigorously stirred for 24 h, whereas the white Ch-NPs nanoparticles were gradually formed. After centrifugation at 5000 rpm, the Ch-NPs nanoparticles were separated, washed with 30% ethanol, 75% ethanol and 100% ethanol solution, respectively. The prepared Ch-NPs were then dispersed in distilled water, and the concentration was determined by drying the solution. The differences in weight determined the concentration.

Ch-NPs characterization

Fourier-transform infrared spectroscopy (FT-IR)

The spectra were collected using the Mattson-Infinity Series Bench Top 961 spectrometer. One milligram of each sample of raw and modified alumina silicate was

ground and specified with a resolution of 2 cm^{-1} in the range of 400–4000 cm^{-1}.

Zeta potential (ζ) and particle size distribution

The particle size and ζ were measured using a Malvern Zetasizer Nano Series (NANO-ZS) HT via dynamic light scattering (DLS) in ethanol. The ζ is the electrostatic potential at the shear plane of a particle and is related to both the surface charge and the local environment of the particle.

High-resolution transmission electron microscopy (TEM)

Images of Ch-NPs nanoparticle images were recorded using a JEM-2100F TEM instrument (JEOL) at an acceleration voltage of 200 kW. Five drops of the solution were diluted in 1 mL of distilled water. The solution was then placed on a carbon-coated copper grid and allowed to evaporate.

Radical-scavenging ability

The 1,1-diphenyl-2-picrylhydrazyl (DPPH) radical-scavenging activity of the prepared Ch-NPs was determined (Bersuder et al. 1998).

Ch-NPs cytotoxicity studies using A549 cells

Cell viability

Cell viability was evaluated using the mitochondrial-dependent reduction of yellow 3-(4,5-dimethylthiazol-2-yl)-2,5-diphenyl tetrazolium bromide (MTT) to purple formazan. A549 cells were grown as monolayers at 37 °C in a 5% CO_2 humidified atmosphere in Dulbecco's Modified Eagle Medium supplemented with 10% fetal bovine serum, 2-mM glutamine, and 100 l g/ml penicillin–streptomycin. Cells were passaged three times per week using trypsin–EDTA and were used for studies after five passages. Absorbance was measured using a microplate multi-well reader (Bio-Rad Laboratories Inc., Model 3350, Hercules, California, USA) at 595 nm and a reference wavelength of 620 nm.

Animals study

Forty Sprague Dawley adult male albino rats 8 weeks old (180–200 g; 190 ± 10 g) obtained from the National Research Center were housed in accordance with the international animal care policies and in compliance with the ethics committee of the center. The study conformed to the "Guide for the Care and Use of Laboratory Animals" by the National Institute of Health (Publication No. 85-23, 1996). Animals were housed in plastic cages and maintained under environmentally controlled light and temperature conditions (constant temperature; 25–27 °C with a 12 h light/dark cycle). The animals were also provided with a standard laboratory pellet diet (15 g/rat/day) and distilled water ad libitum for one week prior to study commencement.

Study design

The animals were randomly divided into four groups (10 rats/group) as follows:

Group 1: The normal control group.

Group 2: The lung fibrosis group. The animals received oral INDOX (600 mg/kg b.w./rat in corn oil) via gavage (Shit et al. 2008).

Group 3: The animals in the positive group were given Ch-NPs orally (2 mg/kg/day) (Sabry et al. 2016).

Group 4: The animals were given Ch-NPs (2 mg/kg/day) orally for another 30 days after the oral administration of INDOX (600 mg/kg per rat).

All animals were humanely euthanized after 30 days post treatment via exsanguination under sodium pentobarbital anesthesia. The blood samples were obtained via sinus orbital puncture and collected in sterile syringes. Furthermore, the samples were centrifuged at 3000 rpm for 10 min to separate serum for biochemical analyses.

Biochemical assays

The superoxide dismutase (SOD), glutathione peroxidase (GPx) (Nishikimi et al. 1972), malondialdehyde (MDA) (Ohkawa et al. 1979), and nitric oxide (NO) serum levels (Miranda et al. 2001) were determined spectrophotometry using kits purchased from Biodiagnostic Co., Egypt. Lung collagen content was assessed biochemically through the determination of hydroxyproline concentration (HYP) using a rat enzyme-linked immunosorbent assay (ELISA) kit (Bioneovan Co., Ltd., Beijing, China) according to the manufacturer's protocols as a biochemical index of fibrosis. Myeloperoxidase (MPO) activity was measured using a rat ELISA kit (Wuhan Fine Biotech Co., Ltd, Wuhan, China) according to the manufacturer's protocols as an indicator of neutrophil infiltration and activation. The cytokeratin-19 (CK-19) serum level was estimated using a rat ELISA kit (Sino Gene Clon. Biotech Co., Ltd) according to the manufacturer's protocols.

RNA extraction and quantitative real-time PCR (q RT-PCR)

RNA was extracted from lung tissue with TRI Reagent (Sigma–Aldrich Inc. USA), and cDNA synthesis was performed with MMLV-reverse transcriptase. q RT-PCR was done with SYBR Green PCR master mix (MBI-Fermentas, Lithuania). The relative quantitative gene expression levels of microRNA-101(MiR-101) and metallopeptidase-9 (MMP-9) in lung tissue were determined. The house keeping gene GAPDH was used as control. The primers used in this study are listed in Table 1. Real-time cycling parameters included initial denaturation (95 °C–5 min), 40 cycles of denaturation at 95 °C for 20 s, annealing at 58 °C for 20 s,

Table 1 Primer sequences for qRT-PCR

Gene	Primer sequence (5′–3′)	References
MiR-101	F: TGCCCTGGCTCAGTTATCAC R: CCTGCTGTGATGAGACTTCTC	Huang et al. (2017)
MMP-9	F: TGTACCGCTATGGTTACACTCG R: GGCAGGGACAGTTGCTTCT	Qu et al. (2019)
GAPDH	F: TGGAGTCTACTGGCGTCTTCAC R: GGCATGGACTGTGGTCATGA	Qu et al. (2019)

F: forward primer; R: reverse primer, metallopeptidase-9 (MMP-9), microRNA-101 (MiR-101)

and extension at 68 °C for 20 s followed by a melting curve analysis for the conformation of the specificity of PCR. The experiment was performed in Master cycler ep realplex 2 system (Eppendorf AG, Germany). All the experiments were performed in triplicates.

The reaction parameters were denaturation at 95.0 °C for 15 s; annealing at 55.0 °C for 30 s; and extension at 72.0 °C for 30 s. At study end, a melting curve was generated at 95.0 °C to check the primer quality. Gene expression was calculated using the formulas from Bio-Rad Laboratories Inc.

Cytotoxicity studies

The MTT assay was used to assess in vitro cytotoxic effects of free Ch-NPs in A549 lung cancer cells. The cells were grown at 37 °C plus 5% CO_2 under controlled humidity conditions (95%) in DMEM plus 10% fetal bovine serum and antibiotics (1 × Penstrip, Invitrogen). The cells were seeded in equal numbers following trypan blue cell counting (5000–8000 cells per well in a 96-well plate). Then, the cells were washed with sterile 1 × PBS and then cultured in serum-free media for 24 h for synchronization. Serial dilutions (10, 20, 40, 80, and 160 µg/mL) of supplied samples were dissolved in phosphate buffer saline (PBS) and DMEM and were added to the plates in triplicate and incubated with samples for 48 h. Then, the culture media were discarded, the cells were washed with 1 × PBS, and 10 µL of MTT was added per well. The plates were incubated for 4 h at room temperature in the dark. Subsequently, the crystals were dissolved in dimethyl sulfoxide (100 µL), and the plates were processed using a microplate reader at 570 nm. The cells without treatments were used as negative controls**.** Cell viability (percentage) at different concentrations was calculated using the following equation:

$$\%\ \textbf{Cell viabilities} = \text{absorbance of treated cells} / \text{absorbance of control cells} \times 100$$

Histopathology

Lung specimens were fixed in 10% neutralized formalin for 24 h using standard dehydration and paraffin wax embedding procedures. The sections (5-µm) were cut using a microtome, collected on poly lysine glass slides, and stained with hematoxylin and eosin (H&E) (Carleton 1976). The slides were histopathologically examined using a light microscope.

Immunohistochemistry

For immunohistochemical staining, 5-µm lung slices were deparaffinized in xylene, hydrated in a graded alcohol series, and washed with 1% phosphate-buffered saline (PBS pH 7.0). Then, the slices were incubated in 10-mmol/L citrate buffer (pH 6.0) at 100 °C for 10 min for antigen retrieval and then placed in 3% hydrogen peroxide (H_2O_2) for 15 min at room temperature to block endogenous peroxidase activity. After rinsing three times in 1% PBS, the sections were blocked in goat serum for 30 min and incubated with a rabbit polyclonal primary antibody against cyclooxygenase-2 (COX-2; 1:100. Wanlei Life Sciences, Shenyang, China) at 4 °C overnight. The sections were then washed with 1% PBS, incubated with a corresponding goat anti-rabbit biotin-labeled secondary antibody (1:200; Beyotime, Shanghai, China) at 37 °C for 30 min, and subsequently incubated in avidin–horseradish peroxidase complex (Beyotime). The sections were then visualized using 3,3′-diaminobenzidine (SolarBio, Beijing, China) and counterstained with hematoxylin and eosin (H&E) (SolarBio) (Bancroft et al. 1996**).**

Statistical analysis

All statistical analyses were conducted using the statistical package for Windows Version 21 (SPSS Software, Chicago, IL, USA). The results for continuous variables were expressed as mean ± standard error (SE). The values were compared using one-way analysis of variance. Post hoc testing was conducted for inter-group comparisons using the least significant difference test, and p values < 0.05 were considered statistically significant (Armitage et al. 2001).

Results

FT-IR spectroscopy results

The FT-IR analysis of Ch-NPs nanoparticles is presented in Fig. 1. Functional groups and capping ligands were investigated to evaluate the stability of biosynthesized polymeric nanoparticles. A peak at 3444 cm^{-1} was attributed to the symmetric stretching vibration of OH; this region was matched with N–H and O–H stretching. A peak at 2920 cm^{-1} was attributed to the symmetric and asymmetric stretch of CH_3 and CH_2. The peak at 1627 cm^{-1} referred to the C–O secondary amide stretch. The peak at 1384 cm^{-1} was attributed to CH_3 in the $NHCOCH_3$ group. The peak at approximately 1095 cm^{-1} was attributed to C–O in the secondary OH group. The

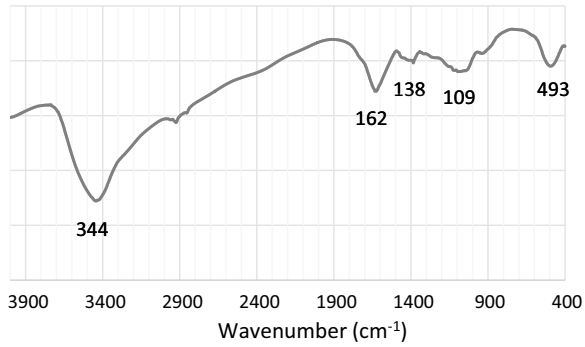

Fig.1 FT-IR spectra of Ch-NPs-TPP nanoparticles

peak at 910 cm^{-1} was attributed to the characteristic bands of TPP poly anions. Chitosan TPP nanoparticles were produced using the ionic gelatin method via complexation between positively charged amino groups and negatively charged polyanions (Abuelmakarem et al. 1987).

Zeta potential analysis

Zeta potential studies indicated surface charges on particles. It was measured to determine nanoparticle stability in the suspension solution. The chitosan particles in acetate buffer solution had a high positive zeta potential owing to the protonation of amino groups as NH_3^+. The zeta potential for Ch-NPs nanoparticles was produced at two peaks (−5 and 30 mv) (Fig. 2). The negative zeta potential was due to the neutralization of protonated amino groups with polyanions. Chitosan had a high positive zeta potential means that there is on the surface of nanoparticles a net positive charge. This indicated that Ch-NPs were highly stable in solution. The positive charges generated electrostatic repulsion forces between linear chitosan chains. In addition, inter-hydrogen bonds were formed between the amino and hydroxyl groups of chitosan with hydroxyl groups or oxygen atoms of water (Hejjaji et al. 2017).

DLS analysis

The particle size distribution of Ch-NPs nanoparticles is presented in Fig. 3, and the average size of Ch-NPs nanoparticle was approximately 121 nm. Aggregated particles were identified using TEM imaging. DLS detected the aggregated nanoparticles as a particle. The dispersed nanoparticles in the liquid phase were aggregated due to strong cross-linking.

TEM analyses

Ch-NPs TEM images at 50- and 200-nm resolution are presented in Fig. 4. The images show roughly spherical self-assembled structures (Sreekumar et al. 2018).

Ch-NPs antioxidant activity

Chitosan was significantly scavenged by DPPH radicals to reach the maximum inhibition percentage, at approximately 750 and 1000 µg/mL, respectively (Table 2). The nanoparticles were most effective in the decolorization of reaction mixture than the two tested standards at these high concentrations, whereas it showed the lowest effect at 100 and 250 µg/mL, respectively. Therefore, the radical-scavenging activity was concentration-dependent.

Cytotoxicity results

The results shown in Fig. 5 demonstrated that the A549 cells treated with Ch-NPs-TPP showed an IC50 value of 91.5 µg/mL within 48 h, Ch-NPs facilitated intracellular uptake through electrostatic attraction, as Ch-NPs carrying positive charges tended to combine with the negatively charged cell-surface proteins.

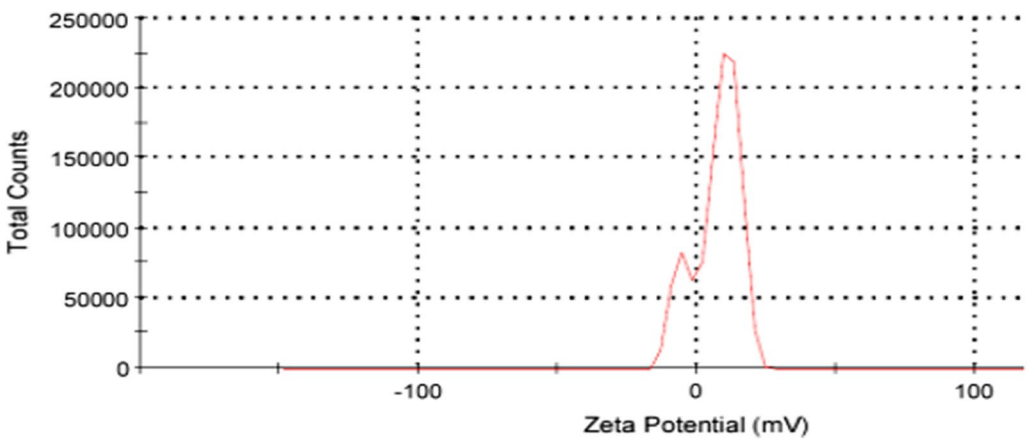

Fig. 2 Zeta potential of Ch-NPs-TPP

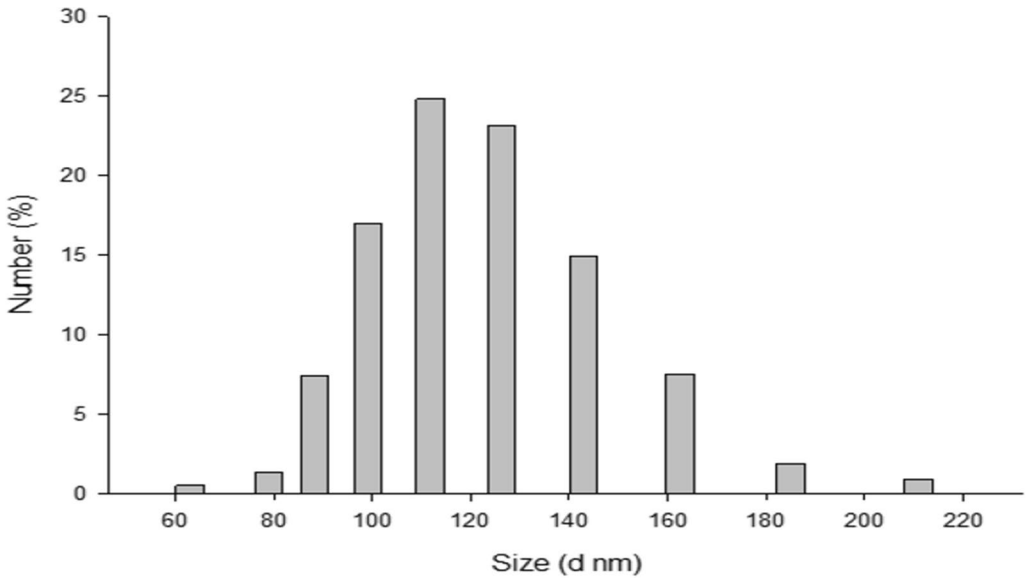

Fig. 3 Ch-NPs particle size distribution

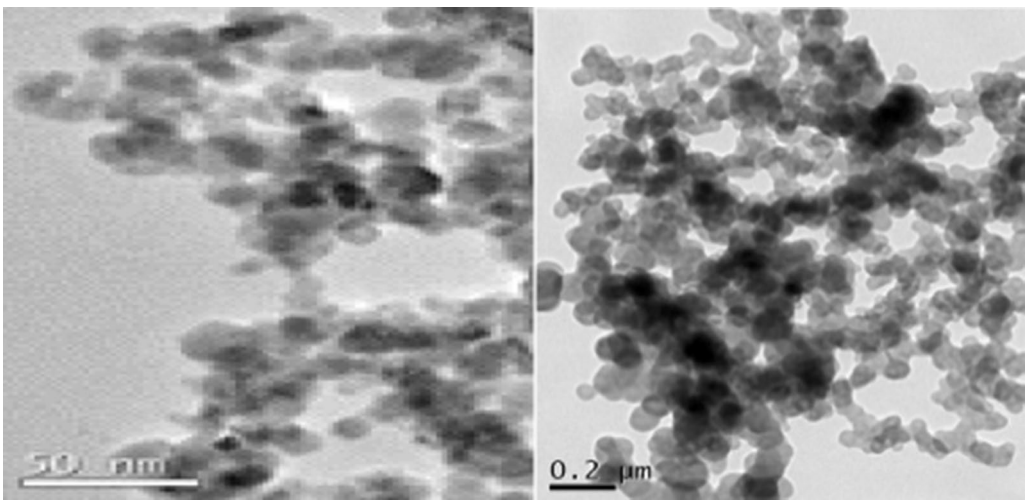

Fig. 4 TEM Ch-NPs—micrographs at 50- and 200-nm resolution

Table 2 Ch-NPs antioxidant activity

Concentration	100 µg/mL	250 µg/ml	500 µg/ml	750 µg/mL	1000 µg/mL
Chitosan	47.9	69.5	79.8	98.4	100

Biochemical results

The MDA and NO serum levels at $P<0.05$ were greatly increased in INDOX-administered animals when compared with the normal control group (referring to elevated oxidative stress) (Table 3). Contrarily, oral administration of Ch-NPs normalized the NO and MDA serum levels when compared with the INDOX group.

Also, INDOX-administered rats exhibited significantly decreased SOD and GPx activities when compared with the control group (Table 4). Contrarily, oral administration of Ch-NPs improved the SOD and GPx activities when compared with the INDOX-administered group, whereas the activities remained significantly low in the control group.

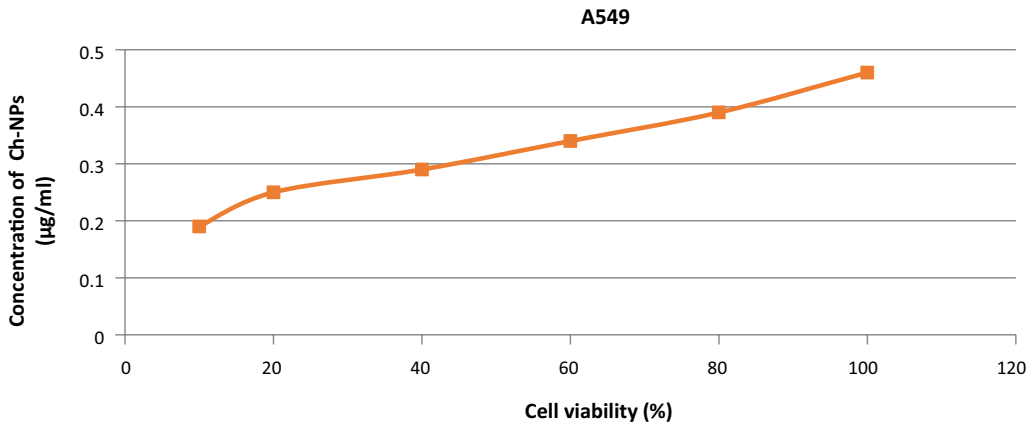

Fig. 5 Ch-NPs cytotoxicity toward A549 cells

Table 3 The effect of Ch-NPs on the NO and MDA serum levels in rats

Parameters	Groups	
	NO (µmol/L)	MDA (µmol/L)
1- Control	5.77 ± 0.97	15.10 ± 0.96
2- INDOX	9.50 ± 0.37[a]	24.13 ± 2.14[a]
3- Ch-NPs	3.07 ± 0.94[b]	11.12 ± 0.44[b]
4- INDOX + Ch-NPs	5.98 ± 0.29[b]	17.38 ± 0.45[b]

Values are expressed as mean ± standard error (SE) (10 rats/group)

[a] Significant changes when compared with the group 1 at $P < 0.05$

[b] Significant changes when compared with the INDOX group at $P < 0.05$

Table 4 The effects of Ch-NPs TPP on the SOD and GPx serum levels in rats

Groups	Parameters	
	SOD (U/mL)	GPx (U/mL)
Control	6.27 ± 0.62	79.58 ± 3.08
INDOX	1.24 ± 0.33[a]	28.65 ± 0.81[a]
Ch-NPs	7.87 ± 0.87[b]	78.82 ± 2.06[b]
INDOX + Ch-NPs	3.30 ± 0.39[b]	65.28 ± 3.37[b]

Values expressed as mean ± standard error (SE) (10 rats/group)

[a] Significant changes when compared with the control group at $P < 0.05$

[b] significant changes when compared with the INDOX group at $P < 0.05$

Our data also indicated that INDOX-administered rats had significant CK-19, HYP, and MPO serum levels when compared with control animals (Fig. 6). Contrarily, Ch-NPs treatment significantly inhibited the CK-19, HYP, and MPO serum levels ($P < 0.05$) when compared with INDOX-administered animals.

We also measured the MMP-9 and MiR-101 gene expression levels in the lung tissue via qRT-PCR. When

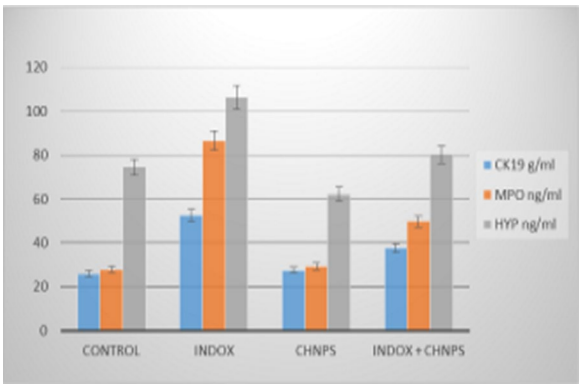

Fig. 6 The effects of Ch-NPs on the CK-19, MPO, and HYP serum levels in rats administered INDOX

compared with control animals, the levels of MMP-9 and MiR-101 (Fig. 7) were significantly ($P < 0.05$) upregulated in the INDOX group. Contrarily, Ch-NPs-TPP administration resulted in a significant downregulation of MMP-9 and MiR-101 levels (Fig. 7, $P < 0.05$) when compared with the INDOX group only.

Histopathological and immunohistochemical examinations

Microscopic investigation of the lung tissue sections of the untreated control group revealed that the main lung tissue architecture was normal (Fig. 8, Table 5). In INDOX-administered animals, we observed a proliferation of fibrous tissue bundles around lung capillaries and interstitial tissues associated with inflammatory cells (Fig. 9, Table 5). For rats treated with Ch-NPs, a diffused focal proliferation of inflammatory cells was associated with fibrous tissue proliferation (Fig. 10, Table 5). In addition, rats pre-treated with Ch-NPs and treated with INDOX demonstrated diffused focal proliferation of

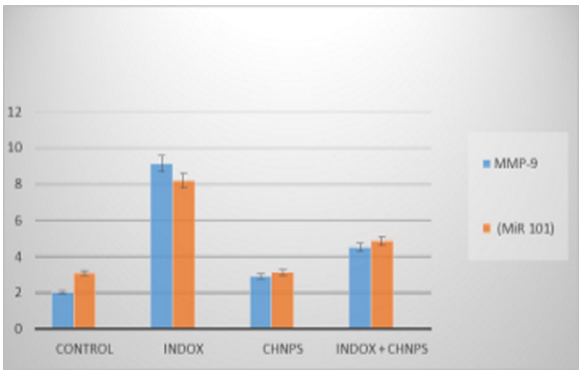

Fig. 7 The effects of Ch-NPs on the MMP-9 and MiR-101 gene expression levels in rats treated with INDOX

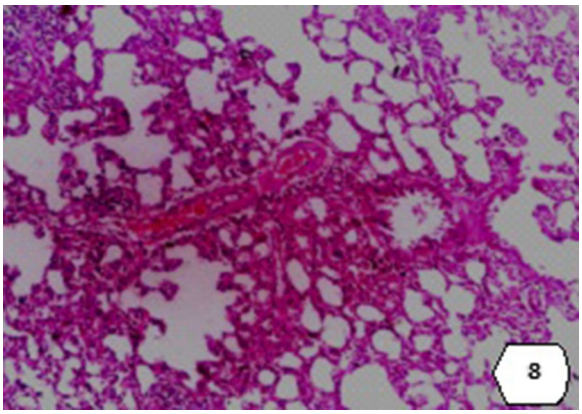

Fig. 8 Lung tissue image of normal control rats showing normal lung architecture (hematoxylin and eosin × 100 magnification)

Table 5 The modulatory effect of Ch-NPs on lung tissue in the study groups

Groups	Control	INDOX	Ch-NPs	INDOX + Ch-NPs
Fibrous tissue proliferation	−	+++	+	+
Inflammatory reaction	−	+++	++	++
Basophilic cell infiltration	−	−	+++	++
Enzymatic reaction	−	+++	+	++

− negative, + mild, ++ moderate and +++ severe reaction

inflammatory cells associated with fibrous tissue proliferation (Fig. 11, Table 5).

Also, immunohistochemical examinations revealed that control rat sections showed negative COX-2 staining reactions (Fig. 12). However, in INDOX-administered animals, marked positive COX-2 staining reactions around lung capillaries, bronchioles, and

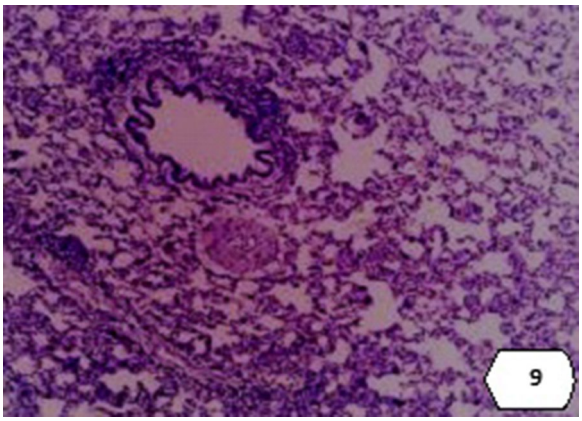

Fig. 9 Lung tissue image of normal control rats showing negative COX-2 immunoreactivity (× 400 magnification)

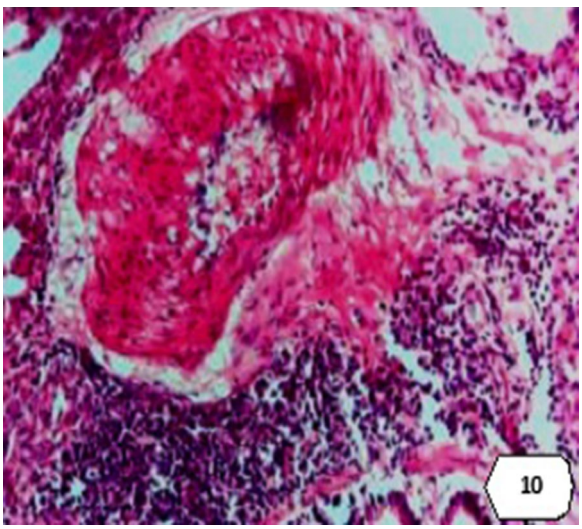

Fig. 10 Lung tissue image of INDOX-administered animals showing the proliferation of fibrous tissue bundles around lung capillaries and interstitial tissues associated with inflammatory cells (star) (hematoxylin and eosin × 400 magnification)

interstitial tissues were observed (Fig. 13). For the Ch-NPs group, moderate positive COX-2 staining around lung capillaries, bronchioles, and interstitial tissues was identified (Fig. 14). Contrarily, the Ch-NPs + INDOX group showed moderate positive COX-2 staining around lung capillaries, bronchioles, and interstitial tissues (Fig. 15).

Discussion

The unique features of NPs make them highly attractive for a wide variety of medical and biological applications. In this study, we evaluated the therapeutic role of Ch-NPs against lung fibrosis in INDOX-administered rats.

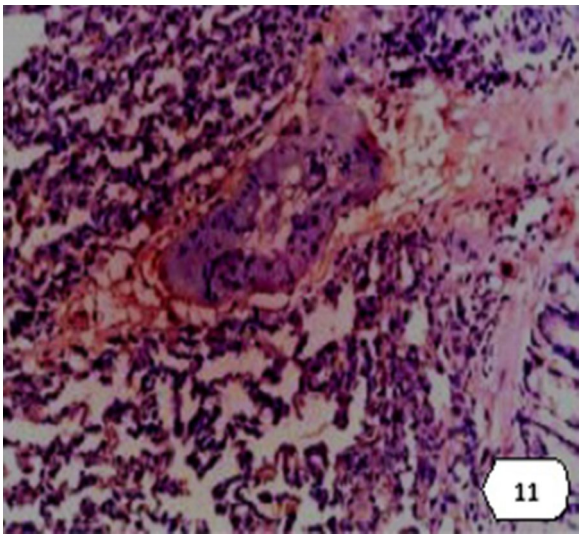

Fig. 11 Lung tissue image of INDOX-administered animals showing mild positive COX-2 immunoreactivity around lung capillaries, bronchioles, and interstitial tissues (× 400 magnification)

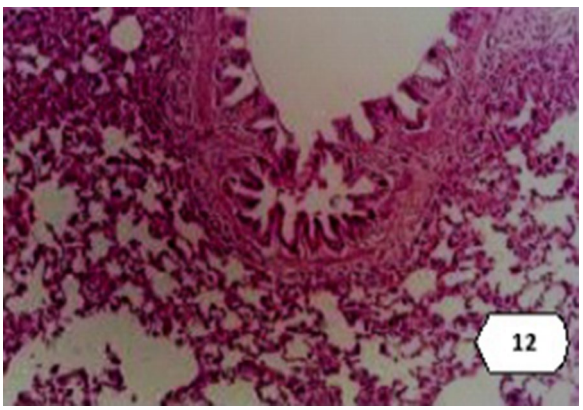

Fig. 12 Lung tissue image of Ch-NPs animals showing diffused focal proliferation of inflammatory cells associated with fibrous tissue (hematoxylin and eosin × 200 magnification)

Oxidative stress has an important role during PF pathogenesis (Cheresh et al. 2013). We demonstrated that the MDA and NO serum levels were significantly increased in INDOX-administered rats, accompanied by reductions in both SOD and GPx enzyme activities levels. Contrarily, Ch-NPs significantly reduced the MDA and NO serum levels and increased endogenous SOD and GPx levels. These data suggested that INDOX increased the MDA and NO serum levels and stimulated oxidative stress. Our findings correlated with those of Yeh et al. (2006) who reported that exposure to parquet (PQ) increases the NO and MDA levels in lung epithelial cells.

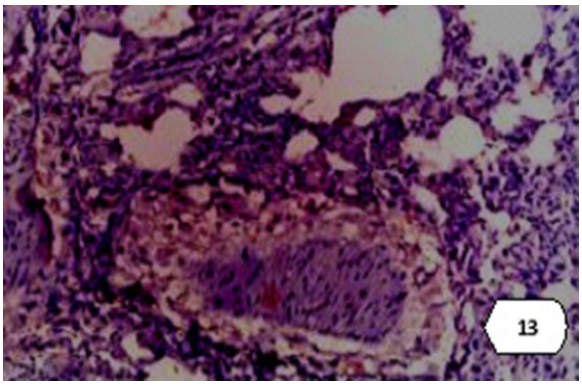

Fig. 13 Lung tissue image of Ch-NPs animals showing moderate positive COX-2 immunoreactivity around lung capillaries, bronchioles, and interstitial tissues (× 200 magnification)

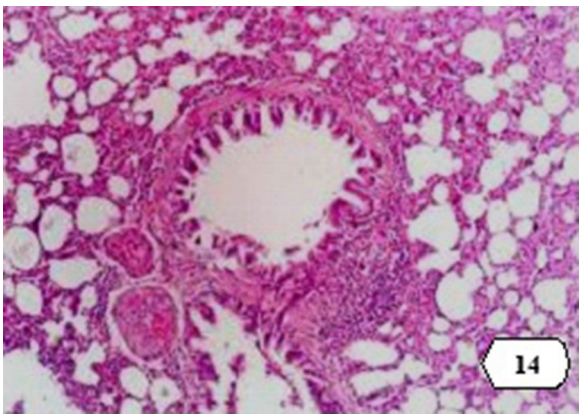

Fig. 14 Lung tissue image of Ch-NPs + INDOX animals showing diffused focal proliferation of inflammatory cells associated with fibrous tissue proliferation (hematoxylin and eosin × 200 magnification)

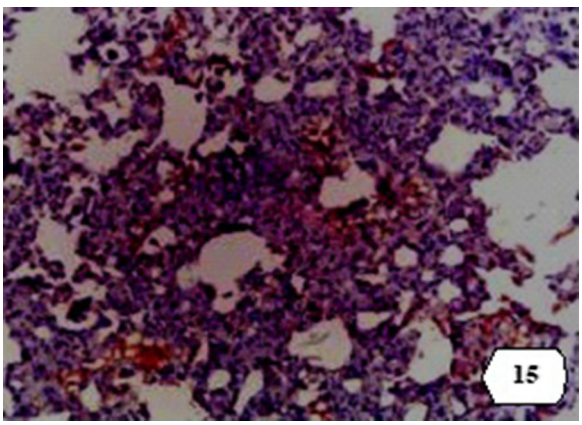

Fig. 15 Lung tissue image of Ch-NPs + INDOX animals showing moderate positive COX-2 immunoreactivity (× 200 magnification)

According to our data, significant improvements in MDA and NO levels after Ch-NPs administration may have been due to their potent antioxidative activities. Our findings agreed with those of Wu et al. (2015) who reported that Ch-NPs exerted curative effects on cell membrane integrity by inhibiting lipid peroxidation through its antioxidant property, or due to its ability to inhibit accumulation of lipid by its antilipidemic property (Yeh et al. 2006). We also observed that the SOD and GPx activity levels were significantly reduced in INDOX-administered animals when compared with control animals. Our results were consistent with those of Mirmalek et al. (2016) who suggested that these reductions may have been due to enhanced lipid peroxidation, or inactivation and depletion of antioxidative enzymes levels due to high doses of INDOX. Moreover, Mudaraddi et al. (2012) suggested that INDOX decreased GSH levels in mice may be due to the fact that INDOX is a fluorinated compound prone to bind various antioxidants and antioxidation enzymes.

In this context, it was clear that Ch-NPs treatment significantly promoted SOD and GPx activities to near-normal control levels. Interestingly, Wardani and Eraiko (2018) demonstrated that Ch-NPs administration increased SOD and GPx activities in gastric cadmium-treated rats, which might be due to the capability of Ch-NPs to decrease the accumulation of free radicals by its free-radical quenching property that serves to reduce H_2O_2-induced oxidative damage to tissue and restore the activities of endogenous antioxidants, including SOD and GPx enzyme levels**.** Moreover**,** Wen et al. (2013) reported that Ch-NPs restored the SOD and GPx activities by increasing their gene expression levels.

Inflammation responses are key mechanisms during PF pathogenesis and are characterized by the elevated proliferation of endogenous and inflammatory cells. These cells, together with lung epithelial and endothelial cells, activate alveolar and interstitial macrophages Friedman and Junega (2010). Neutrophil infiltration into the lung tissues is evaluated by MPO **(**Babior et al. 1997**).** We observed that INDOX administration increased the MPO activity when compared with normal control animals, whereas Ch-NPs alleviated the activity to near-normal levels. Our results agreed with those of Zhang et al. (2016) who observed that Ch-NPs significantly inhibited the MPO activity; the reason could be related to the good anti-inflammatory activities of chitosan.

The degree of PF was measured using HYP levels, as severely affected myofibroblast proliferation leads to considerable collagen deposition **(**Kim et al. 2014**).** Ch-NPs promoted collagen fiber growth by inhibiting HYP serum levels **(**Xin et al. 2019**).**

Altaib et al. (2017) demonstrated that COX-2 and COX metabolites were involved in the progression and development of acute lung injury in animal models. In the present setup, we demonstrated severe immunopositive COX-2 expression in bronchial epithelium regions of INDOX-administered rat lungs when compared with control animals. These findings correlated with those of Yeh et al. (2006) who concluded that PQ-exposure upregulated COX-2 expression and hypothesized that INDOX, by disturbing the antioxidant status, increased pro-inflammatory factors, such as NO, which in turn led to lung cell inflammation **(**Kaur et al. 2016**).** Our findings supported the hypothesis that significant positive COX-2 expression in INDOX-administered rat lungs confirmed that inflammation was associated with histopathological, inflammatory, and biochemical changes.

However, we revealed moderate immune positive COX-2 expression around lung capillaries, bronchioles, and interstitial tissues in the Ch-NPs-treated groups. Our findings agreed with those of Nam et al. (2007) and Adhikari and Yadav, (2018) who demonstrated that chitosan inhibited pro-inflammatory cytokine-induced invasiveness in HT-29 cells and consequently induced COX-2 expression. Also, chitosan triggered AMPK activity, which in turn prevented TNF-α induced NF-κB signaling and COX-2 and iNOS expression in both rabbit and human synoviocytes **(**Kunanusornchai et al. 2016**).**

MMPs can degrade and remodel the extracellular matrix, which are believed to play an important role in the development of fibrotic tissue. The present setup demonstrated that the oral administration of INDOX to rats significantly upregulated the gene expressions of both MMP-9 and MiR-101. These data agreed with the findings of Lui et al. (2016) who reported that PQ treatment markedly upregulated miR-21 expression, stimulated FSTL1 expression, facilitated TGF-β/Smad2 and p38MAPK signal transduction, and finally induced PF. We hypothesize that pesticides have impacts on micro RNAs including MiR-101.

Similarly, we demonstrated that treatment of the INDOX-administered group with Ch-NPs significantly downregulated the gene expressions of MMP-9 and MiR-101. These findings are in agreement with those of Wardani and Eraiko (2018) who speculated that chitosan exhibited several biological activities, including antioxidant, MMP-inhibitory, and anti-inflammatory activities.

Microscopic investigation of the lung tissue from INDOX-administered animals showed a proliferation in fibrous tissue bundles around lung capillaries and interstitial tissues associated with inflammatory cells. Our histopathology data agreed with the findings of Kaur et al. (2016) who reported that exposure to 2-mg INDOX-induced peribronchial infiltration of inflammatory cells

and thickening of alveolar septa. Also, Liu et al. (2016) showed considerable inflammatory cell infiltration damage and thickening in the alveolar walls in the lung sections from PQ-exposed rats. Moreover, Altaib et al. (2017) suggested that bleomycin was associated with cellular infiltration surrounding bronchioles and interalveolar septa.

The histopathology of lung tissue sections in animals pre-treated with Ch-NPs showed a normal appearance. Our findings agreed with those of Zhou et al. (2014) who suggested that chitosan exhibited potent antifibrotic activities by reducing fibroblast proliferation, decreasing extracellular matrix deposition and collagen synthesis levels. In addition, chitosan was shown to stimulate reepithelialization in experimental wounds (Lee et al. 2016a, b).

We confirmed that Ch-NPs exhibited anticancer activities, as indicated by our in vitro studies of A549 cells. These findings agreed with those of Karagozlu and Kim (2014) who speculated that Ch-NPs exerted antitumor roles by interfering with cell metabolism, reducing growth, and enhancing apoptosis.

Conclusions

In vivo and in vitro model treatment with Ch-NPs improved antioxidant activities and reduced oxidative stress levels, as indicated by increased antioxidant (SOD and GPx) and decreased MDA and NO levels. Thus, Ch-NPs may exert therapeutic actions against INDOX-induced lung fibrosis in rats, possibly via antioxidant and anti-inflammatory mechanisms. Therefore, Ch-NPs may be viable natural products for counteracting INDOX—poisoning.

Abbreviations

Ch-NPs: Chitosan nanoparticles; COX-2: Cyclooxygenase-2; CK-19: Cytokeratin-19; DLS: Dynamic light scattering:; FT-IR: Fourier-transform infrared spectroscopy; GPx: Glutathione peroxidase; HYP: Hydroxyproline; INDOX: Indoxacarb; MDA: Malondialdehyde; MMP-9: Matrix metallopeptidase-9; MiR-101: MicroRNA-101; MPO: Myeloperoxidase; NO: Nitric oxide; PF: Pulmonary fibrosis; q RT-PCR: Quantitative real-time PCR; SOD: Superoxide dismutase; TEM: Transmission electron microscopy.

Acknowledgements

This work was supported by the National Research Center [Internal project No. 110501].

Author contributions

NA and SH designed and performed the experiment, responsible for all the physiological, biochemical, and statistical analyses, and wrote and reviewed the manuscript. MS and M. designed and synthesized nanoparticles, statistical analysis and wrote and reviewed the manuscript. MShS. All authors read and approved the final manuscript.

Funding

There are currently no funding sources in the design of the study and collection, analysis and interpretation of data, and in writing of the manuscript.

Availability of data and materials

The datasets generated and/or analyzed during the current study are included in this published manuscript.

Declarations

Ethics approval and consent to participate

National Research Centre-Egypt, Medical Research Ethics Committee, Registration Number-18172.

Consent for publication

Not applicable.

Competing interests

The authors declare that they have no known competing financial interests or personal relationships that could have appeared to influence the work reported in this paper.

Author details

[1]Hormones Department, Medical Research and Clinical Studies Institute, National Research Centre, 33-El-Bohouth St. (Former El-Tahrir St.), Dokki, Giza P.O 12622, Egypt. [2]Petrochemical Department, Egyptian Petroleum Research Institute, Nasr City, Egypt.

Received: 5 November 2021 Accepted: 14 November 2022
Published online: 27 November 2022

References

Abuelmakarem HS, Sliem MA, El-Azab J, Farghaly MMA, Ahmed WA (1987) Toward highly efficient cancer imaging and therapy using the environment-friendly chitosan nanoparticles and NIR laser. Biosensors 9(1):28. https://doi.org/10.3390/bios9010028

Adhikari HS, Yadav PN (2018) Anticancer activity of chitosan, chitosan derivatives, and their mechanism of action. Int J Biomater ID 2952085. https://doi.org/10.1155/2018/2952085

Alavanja MC (2009) Introduction: pesticides use and exposure, extensive worldwide. Rev Environ Health 24(4):303–310. https://doi.org/10.1515/reveh.2009.24.4.303

Altaib ZM, Mansy AE, Elmahlawy AM, Sabry D (2017) The possible ameliorative effect of mesenchymal stem cells and curcumin on bleomycin induced lung injuries in the adult male rats: histological and immunohistochemical study. J Stem Cell Res Ther 7:389. https://doi.org/10.4172/2157-7633.1000389

Armitage P, Berry G, Mathews JNS (2001) Statistical method in medical research, 2nd edn. Blockwell Significant Publication, Oxford, pp 186–213

Babior BM, Benna JE, Chanock SJ, Smith RM (1997) The NADPH oxidase of leukocytes: the respiratory burst oxidase. Cold Spring Harbor Monogr Arch 34:737–783. https://doi.org/10.1101/0.737-783

Bancroft JD, Stevens A, Dawswon MP (1996) Theory and practice of histological techniques. In: 4th ed. Churchill Livingstone, Edinbergh, London and New York, pp 273–292. ISBN: 978-0-7020-6864-5

Bersuder P, Hole M, Smith GJ (1998) Antioxidants from a heated histidine-glucose model system. I. Investigation of the antioxidant role of histidine and isolation of antioxidants by high-performance liquid chromatography. Am Oil Chem Soc 75:181–187. https://doi.org/10.1007/s11746-998-0030-y

Bolognesi C (2003) Genotoxicity of pesticides: a review of human biomonitoring studies. Mutat Res 543(3):251–272. https://doi.org/10.1016/s1383-5742(03)00015-2

Carleton H (1976) Carleton's histological technique. In: The 4th Ed London Oxford University Press, New York Toront

CEPA (2004) Summary of toxicology data: indoxacarb. In: Department of Pesticide Regulation Medical Toxicology Branch; U.S. EPA. Factsheet: Indoxacarb. Office of Prevention, Pesticides and Toxic Substances., Washington DC. NewYork State Department of Environmental Conservation. Indoxacarb (Avaunt) NYSDEC Registration Letter 3/02. In: E.I. du Pont deNemours and Company, I., & (DuPont Crop Protection), eds. NYC

Cheresh P, Kim SJ, Tulasiram S, Kamp DW (2013) Oxidative stress and pulmonary fibrosis. Biochim Biophys Acta 1832:1028–1040. https://doi.org/10.1016/j.bbadis.2012.11.021

Cheung RCF, Ng TB, Wong JH, Chan WY (2015) Chitosan: an update on potential biomedical and pharmaceutical applications. Mar Drugs 13:5156–5186. https://doi.org/10.3390/md13085156

Du Bois RM (2010) Strategies for treating idiopathic pulmonary fibrosis. Nat Rev Drug Discov 9(2):129. https://doi.org/10.1038/nrd2958

Lee E, Park SJ, Lee JH, Kim MS, Kim CH (2016a) Preparation of chitosan–TPP nanoparticles and their physical and biological properties. Asian J Pharm Sci 11:166–167. https://doi.org/10.1016/j.ajps.2015.11.065

EPA US (2007) Indoxacarb; pesticide tolerance. In: Office of Prevention Pesticides and Toxic Substances, ed: Federal Registrar EPA-HQOPP- 2005-0149; FRL-8137-8:37633-37641.

Friedman M, Juneja VK (2010) Review of antimicrobial and antioxidative activities of chitosans in food. J Food Prot 73:1737–1761. https://doi.org/10.4315/0362-028x-73.9.1737

Hejjaji EM, Smith AM, Morris GA (2017) Designing chitosan-tripolyphosphate microparticles with desired size for specific pharmaceutical or forensic applications. Int J Biol Macromol 95:564–573. https://doi.org/10.1016/j.ijbiomac.2016.11.092

Hock WK, Lorenz ES (2006) Pesticide safety fact sheet: toxicity of pesticides. The Pennsylvania State University, 112 Agricultural Administration Building, University Park, PA 16802

Huang C, Xiao X, Yang Y, Mishra A, Liang Y, Zeng X, Yang X, Xu D, Blackburn MR, Henke CA, Liu L (2017) Micro RNA-101 attenuates pulmonary fibrosis by inhibiting fibroblast proliferation and activation. J Biol Chem 292(40):16420–16439. https://doi.org/10.1074/jbc.M117.805747

Hussein M, El-Hady M, Sayed W, Hefni H (2012) Preparation of some chitosan heavy metal complexes and study of its properties. Polym Sci Ser A 54:113–124. https://doi.org/10.1134/S0965545X12020046

Joshi DP, Mehta NK, Shah JS, Shah VH, Upadhyay UM (2010) Chitosan nanospheres as potential carrier delivery of pharmaceutical API's. Int J Pharm Phytopharmacol Res 2(1):60–65

Karagozlu MZ, Kim SK (2014) Anticancer effects of chitin and chitosan derivatives. Adv Food Nutr Res 72:215–225. https://doi.org/10.1016/B978-0-12-800269-8.00012-9

Kaur S, Mukhopadhyay CS, Sethi RS (2016) Chronic exposure to indoxacarb and pulmonary expression of toll-like receptor-9 in mice. Vet World 9(11):1282–1286. https://doi.org/10.14202/vetworld.2016.1282-1286

Kerch G (2015) The potential of chitosan and its derivatives in prevention and treatment of age-related diseases. Mar Drugs 13:2158–2182. https://doi.org/10.3390/md13042158

Kim SJ, Kim JM, Shim SH, Chang HI (2014) Anthocyanins accelerate the healing of naproxen-induced gastric ulcer in rats by activating antioxidant enzymes via modulation of Nrf2. J Funct Foods 7(1):569–579. https://doi.org/10.1016/j.jff.2013.12.028

Kliment CR, Oury TD (2010) Oxidative stress, extracellular matrix targets, and idiopathic pulmonary fibrosis. Free Radical Biol Med 49(5):707–717. https://doi.org/10.1016/j.freeradbiomed.2010.04.036

Kunanusornchai W, Witoonpanich B, Tawonsawatruk T, Pichyangkura R, Chatsudthipong V, Muanprasat C (2016) Chitosan oligosaccharide suppresses synovial inflammation via AMPK activation: an in vitro and in vivo study. Pharmacol Res 113(Pt A):458–467. https://doi.org/10.1016/j.phrs.2016.09.016

Lee C, Seo J, Ha S, Thao LQ, Lee S, Lee ES, Lee EH, Choi HG, Youn YS (2016b) Treatment of bleomycin-induced pulmonary fibrosis by inhaled tacrolimus-loaded chitosan-coated poly (lactic-co-glycolic acid) nanoparticles. Biomed Pharmacother 78:226–233. https://doi.org/10.1016/j.biopha.2016.01.027

Liu MW, Liu R, Wu HY, Li YY, Su MX, Dong MN, Zhang W, Qian CY (2016) Radix puerariae extracts ameliorate paraquat-induced pulmonary fibrosis by attenuating follistatin-like 1 and nuclear factor erythroid 2p45-related factor-2 signaling pathways through downregulation of miRNA-21 expression. BMC Complement Altern Med 16:11. https://doi.org/10.1186/s12906-016-0991-6

Luo Y, Wang Q (2013) Recent advances of chitosan and its derivatives for novel applications in food science. J Food Process Beverages 1(1):1–3

Mazzotta E, De Benedittis S, Qualtieri A, Muzzalupo R (2019) Actively targeted and redox responsive delivery of anticancer drug by chitosan nanoparticles. Pharmaceutics 12(1):26. https://doi.org/10.3390/pharmaceutics12010026

Miranda KM, Espey MG, Wink DA (2001) A rapid, simple spectrophotometric method for simultaneous detection of nitrate and nitrite. Nitric Oxid 5:62–71. https://doi.org/10.1006/niox.2000.0319

Mirmalek SA, Boushehrinejad AG, Yavari H, Kardeh B, Parsa Y, Salimi-Tabatabaee SA, Yadollah-Damavandi S, Parsa T, Shahverdi E, Jangholi E (2016) Antioxidant and anti-inflammatory effects of coenzyme Q_{10} on L-ARG-induced acute pancreatitis in rat. Oxid Med Cell Longev 2016:5818479. https://doi.org/10.1155/2016/5818479

Moran N (2011) p38 kinase inhibitor approved for idiopathic pulmonary fibrosis. Nat Biotechnol 29:301. https://doi.org/10.1038/nbt0411-301

Mudaraddi TY, Potadar RR, Kaliwal BB (2012) Indoxacarb induces liver oxidative stress in Swiss Albino Mice. Eur J Exp Biol 2(1):180–186

Nam K, Kim M, Shon Y (2007) Inhibition of proinflammatory cytokine-induced invasiveness of HT-29 cells by chitosan oligosaccharide. J Microbiol Biotechnol 17(12):2042

Nishikimi M, Appaji N, Yogi K (1972) The occurrence of superoxide anion in the reaction of reduced phenazine methosulfate and molecular oxygen. Biochem Biophys Res Commun 46(2):849–854. https://doi.org/10.1016/s0006-291x(72)80218-3

Ohkawa H, Ohishi N, Yagi K (1979) Assay for lipid peroxides in animal tissues by thiobarbituric acid reaction. Anal Biochem 95:351–358. https://doi.org/10.1016/0003-2697(79)90738-3

Qu LC, Jiao Y, Jiang ZJ, Song ZP, Peng QH (2019) Acidic preconditioning protects against ischemia-reperfusion lung injury via inhibiting the expression of matrix metalloproteinase 9. J Surg Res 235:569–577. https://doi.org/10.1016/j.jss.2018.10.034

Sabry SA, Sakr SM, Ibrahim H (2016) Effect of chitosan nanoparticles on haloperidol drug-induced hepatotoxicity in albino rats light and electron microscopic study. J Biosci Appl Res 2(12):771–778

Shit SP, Panghal RS, Kumar V, Rana RD (2008) Acute toxicity and gross behavioural effects of indoxacarbin laboratory animals. Haryana Vet 47:49–51

Sreekumar S, Goycoolea FM, Moerschbacher BM, Rivera-Rodriguez GR (2018) Parameters influencing the size of chitosan-TPP nano- and microparticles. Sci Rep 8:4695. https://doi.org/10.1038/s41598-018-23064-4

Wardani K, Eraiko SA (2018) Sudjarwo, protective activity of chitosan nanoparticle against cadmium chloride induced gastric toxicity in rat. J Young Pharm 10(3):303. https://doi.org/10.5530/jyp.2018.10.67

Wen ZS, Liu LJ, Qu YL, Ou Yang XK, Yang LY, Xu ZR (2013) Chitosan nanoparticles attenuate hydrogen peroxide-induced stress injury in mouse macrophage RAW264.7 cells. Mar Drugs 11:3582–3600. https://doi.org/10.3390/md11103582

Wu N, Wen ZS, Xiang XW, Huang YN, Gao Y, Qu YL (2015) Immuno-stimulative activity of low molecular weight chitosans in RAW264. 7 macrophages. Mar Drugs 13(10):6210–6225. https://doi.org/10.3390/md13106210

Wynn TA, Ramalingam TR (2012) Mechanisms of fibrosis: therapeutic translation for fibrotic disease. Nat Med 18(7):1028. https://doi.org/10.1038/nm.2807

Xin X, Yao D, Zhang K, Han S, Liu D, Wang H, Liu X, Li G, Huang J, Wang J (2019) Protective effects of Rosavin on bleomycin-induced pulmonary fibrosis via suppressing fibrotic and inflammatory signaling pathways in mice. Biomed Pharmacother 115:108870. https://doi.org/10.1016/j.biopha.2019.108870

Yang W, Fu J, Wang T, He N (2009) Chitosan/sodium tripolyphosphate nanoparticles: preparation, characterization and application as drug carrier. J Biomed Nanotechnol 5:591–595. https://doi.org/10.1166/jbn.2009.1067

Yeh ST, Guo HR, Su YS, Lin UJ, Hou CC, Chen HM, Chang MC, Wang JY (2006) Protective effects of N-acetylcysteine treatment post-acute paraquat intoxication in rats and in human lung epithelial cells. Toxicology 223:181–190. https://doi.org/10.1016/j.tox.2006.03.019

Zhang W, Liu K, Li L, Li Y, Sui X, Rao Y, Wu J, Wu Q (2016) Therapeutic effect of low molecular weight chitosan containing sepia ink on ethanol-induced gastric ulcer in rats. Acta Cir Bras 31(12):813–820. https://doi.org/10.1590/S0102-865020160120000006

Zheng Z, Zhang W, Sun W, Li X, Duan CJ, Feng Z, Mansour HM (2013) Influence of the carboxymethyl chitosan anti-adhesion solution on the TGF-β1 in a postoperative peritoneal adhesion rat. J Mater Sci Mater Med 24(11):2549–2559. https://doi.org/10.1007/s10856-013-4981-7

Zhou LL, He XY, Xu FY, Zou BX, Shi X (2014) Chitosan aerosol inhalation alleviates lipopolysaccharide induced pulmonary fibrosis in rats. Exp Lung Res 40:467–473. https://doi.org/10.3109/01902148.2014.948231

Publisher's Note